



INSTITUT DE FRANCE
Académie des sciences

Comptes Rendus

Géoscience

Sciences de la Planète


Hossein Mohammadrezaei, Seyed Ahmad Alavi, Mostafa Ghanadian
and Mohammad R. Ghassemi

**The effects of wrench-dominated basement-involved faults on folding of
overlying strata in the Bahregansar anticline, western Persian Gulf, Iran**

Volume 354 (2022), p. 105-118

<https://doi.org/10.5802/crgeos.105>

© Académie des sciences, Paris and the authors, 2022.
Some rights reserved.

 This article is licensed under the
CREATIVE COMMONS ATTRIBUTION 4.0 INTERNATIONAL LICENSE.
<http://creativecommons.org/licenses/by/4.0/>



*Les Comptes Rendus. Géoscience — Sciences de la Planète sont membres du
Centre Mersenne pour l'édition scientifique ouverte*
www.centre-mersenne.org



Original Article — Tectonics, Tectonophysics

The effects of wrench-dominated basement-involved faults on folding of overlying strata in the Bahregansar anticline, western Persian Gulf, Iran

Hossein Mohammadrezaei^{®*},^a, Seyed Ahmad Alavi[®]^a, Mostafa Ghanadian[®]^b
and Mohammad R. Ghassemi[®]^c

^a Department of Sedimentary Basins and Petroleum, Faculty of Earth Sciences, Shahid Beheshti University, Tehran, Iran

^b Department of Geology, Iranian Offshore Oil Company, Tehran, Iran

^c Research Institute for Earth Sciences, Geological Survey of Iran, 1387835841, Tehran, Iran

E-mails: mohammadrezaeihssein1@gmail.com, h_mohammadrezaei@sbu.ac.ir (H. Mohammadrezaei), a-alavi@sbu.ac.ir (S. A. Alavi), Mostafaghanadian@gmail.com (M. Ghanadian), ghassemi.m.r@gmail.com (M. R. Ghassemi)

Abstract. Basement-involved fault geometry and kinematics has a systematic effect on the structural style of the tectonic setting. In this study, 2D and 3D seismic datasets, well data as well as thickness and depth maps were utilized to consider and reconstruct the characteristics and effects of the wrench-dominated basement-involved fault underlying the Bahregansar anticline, which is a gentle, elongated and NW-SE-trending structure in the NW Persian Gulf, on the nature of its folded strata. Moreover, using the 2D sequential restoration, the deformation of the basement structural features was modelled and analysed for its influence on the reactivation of faulting. The results show that the major basement-involved fault, called the Hendijan–Bahregansar–Nowrooz Fault (HBNF), extends along the NE–SW-trending orientation and consist of several key anticlines. The structural evolution of the Bahregansar anticline has been deeply affected by Turonian folding phase and Pliocene Zagros orogeny associated with the HBNE. In the Upper Cretaceous, the HBNF propagated upward through the overlying sedimentary sequences when the inherited normal fault contractionally reactivated in the sinistral-reverse sense as the transpression zone in response to the Neo-Tethys oceanic plate subduction under the Eurasian plate. In this regard, the NNE–SSW-trending Bahregansar anticline (i.e., Arabian trend) formed as a forced fold. Continuing oblique convergence and associated deformation was accommodated by a change in the HBNF displacement sense from sinistral to dextral movement and buckling of the Bahregansar anticline as a result of the Pliocene Zagros orogeny.

Keywords. Basement-involved fault, Bahregansar anticline, Reactivation, Forced fold, Buckling, Zagros orogeny.

Manuscript received 6th March 2021, revised 16th October 2021, accepted 29th November 2021.

* Corresponding author.

1. Introduction

Basement-involved structures characterized by high-angle uplift are common in the foreland fold-and-thrust belts of many orogens. These structures commonly contain significant hydrocarbon accumulations with most major fields located on the crests of these structures [e.g., Mitra and Mount, 1998, Cooper *et al.*, 2006, Granado *et al.*, 2016, Mohammadrezaei *et al.*, 2020]. Basement-involved structures such as faults, fractures, and shear zones can have a strong influence on the development of brittle and ductile structures and the structural style of a geologic setting. Basement faults inherited from previous rifting events are commonly reactivated during tectonic collision in orogenic belts. They have the capacity to influence the localization of deformation, the distribution of sedimentary facies as well as mechanical variations within the geologic configuration [e.g., Koyi *et al.*, 2008, Wang *et al.*, 2016, Neng *et al.*, 2018]. Most studies of contractional basement-involved deformation of sedimentary sequences have focused on faults that accommodate dominant thrust fault kinematics [e.g., McClay and Ellis, 1987, McClay, 2011, Lacombe and Bellahsen, 2016]. There is limited understanding of the deformation pattern and structural styles associated with basement faults that accommodated wrench-dominated kinematics. Although these little-understood faults have accommodated a minor component of dip slip, the net slip is dominated by a main component of strike-slip faulting. In wrench-dominated settings, reverse and normal faults are predominant as well as strike-slip faults, respectively, depending on the convergence and divergence vector of deforming blocks (or plates). In this regard, understanding the interaction between folding and basement faulting, the effects of detachment units on the distribution of growth strata and the different basement fault activities are fundamental for improving the understanding of the structural evolution of the area and also the distribution and nature of hydrocarbon reservoirs in sedimentary basins.

The Zagros Fold-and-Thrust Belt (ZFTB) is characterized by a tectonic wedge (an asymmetrical sedimentary basin) with NW–SE-trending thrusts and folds which vary in geometry and size from a few to tens or even hundreds of kilometers in length [e.g., Agard *et al.*, 2011, Mouthereau *et al.*, 2012,

Ghanadian *et al.*, 2017b]. The subdivisions of the ZFTB consist of the Dezful Embayment, Izeh Zone, Fars Zone and Lurestan Zone (Figure 1). These zones are bordered by the Hendijan–Bahregansar–Nowrooz Fault (HBNF), Kazerun, High Zagros, Balarud, and Mountain Front faults separating the foreland of the ZFTB into distinct rheological and stratigraphic zones [Pirouz *et al.*, 2011, Mouthereau *et al.*, 2007, 2012, Orang *et al.*, 2018]. Various types of fault-related folds such as detachment, fault-bend, fault-propagation folds as well as forced folds are developed in the ZFTB [e.g., Sattarzadeh *et al.*, 1999, Allen and Talebian, 2011, Ghanadian *et al.*, 2017a]. The Persian Gulf, as an epicontinental shallow sea, is a foreland depression of the ZFTB [Soleimany and Sàbat, 2010] (Figure 1). There are several factors that make the Persian Gulf and its adjacent (onshore) areas one of the richest regions of the world in terms of hydrocarbon resources including the presence of extensive source rocks, excellent carbonate and sandstone reservoirs, good regional seals, continuous sedimentation, and large structural traps [e.g., Konyuhov and Maleki, 2006, Mohammadrezaei *et al.*, 2020].

The four major trends obtained from the structural analysis for basement-involved faults are the Arabian trend (N–S and NNE–SSW), the Zagros trend (NW–SE), the Aulitic trend (NE–SW), and the Tethyan trend (E–W), that control the structural features, such as fractures, faults, folds, tectonic subsidence, and active salt tectonism, of the ZFTB and the Persian Gulf [e.g., Edgell, 1996, Bahroudi and Talbot, 2003, Sepehr and Cosgrove, 2007]. The structures with the Arabian trend such as the HBNF, Kharg-Mish fault and Kazerun fault (Figure 1) are older than other trends [Edgell, 1996]. The NNE–SSW-trending HBNF (Figure 1) is a nearly vertical active fault system with dextral-reverse kinematics which developed through the sedimentary cover along-strike the Arabian trend [Molinario *et al.*, 2004, Mohammadrezaei *et al.*, 2020]. It extends from the northern part of the Dezful Embayment in the Zagros foreland basin towards the north Saudi Arabia [Konyuhov and Maleki, 2006]. Several main detachment horizons (or levels) within the cover including the Middle Miocene Gachsaran evaporates, the Aptian–Albian Kazhdumi shale and the Cambrian Hormuz salt have been very effective on the regional shortening of the Zagros belt and Persian Gulf [Agard *et al.*, 2011, Mohammadrezaei *et al.*, 2020]. Moreover, there are several structural

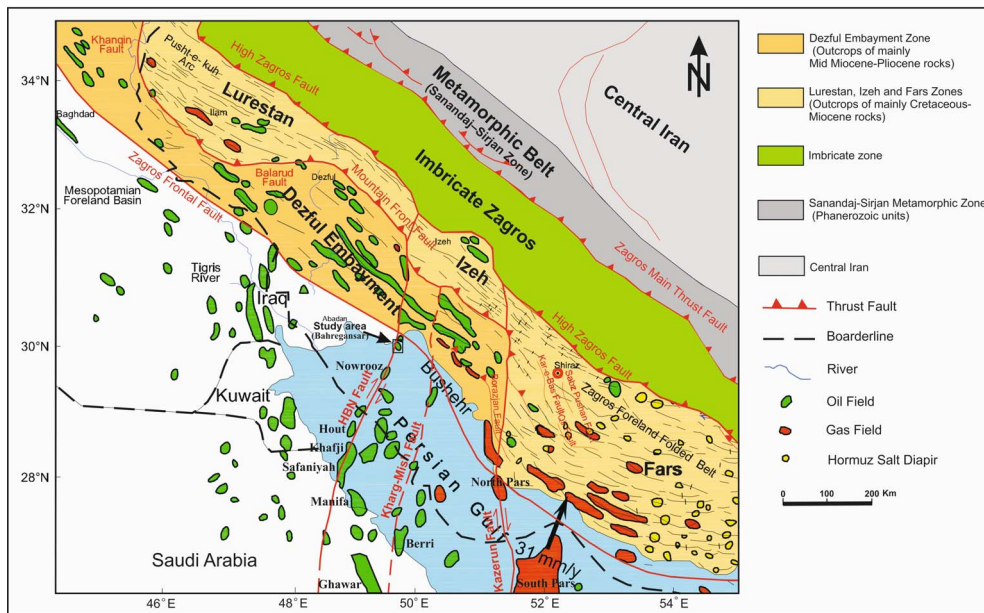


Figure 1. Tectonic setting of the Persian Gulf (a sedimentary basin in the northeastern of the Arabian plate), Zagros fold-and-thrust belt (ZFTB) onshore, and surrounding areas. The map shows the major faults and the main structural subdivisions of the ZFTB, including the imbricate zone, Zagros foredeep zone, and the Zagros foreland folded belt. According to the sedimentary and structural evolution, the Zagros foreland folded belt is subdivided into the Fars, Izeh, Dezful Embayment, and Lurestan domains. The regional distributions of hydrocarbon fields in the ZFTB and surrounding regions have been shown. Modified after Sarkarinejad and Goftari [2019] and Pirouz *et al.* [2011].

anticlinal traps, for example the Bahregansar and Nowrooz anticlines as important hydrocarbon reservoirs (Figure 1), along the HBNE.

Using 2D and 3D seismic datasets, well data as well as depth maps, this study examines how the wrench-dominated basement-involved HBNF affected the overlying sedimentary sequences of the Bahregansar anticline. The purpose of this study are: (1) to provide a detailed account of the geometric and kinematic characteristics of the basement structure; (2) to construct an evolutionary model for the study of the anticline by the 2D sequential restoration across the fold structure; (3) to determine the deformation mechanism for understanding the changes in basement structural features and its influence on the reactivation of faulting; and (4) to investigate the influence of reactivation of a certain basement fault on the fold development in the overlying sedimentary sequences.

2. Tectonostratigraphy of the Bahregansar anticline

The evolution of the ZFTB and Persian Gulf has been affected by main tectonic events of the Arabian plate which contain five major tectonic events from the Precambrian to recent times: (1) the Precambrian compressional event is characterized by the assembly and construction of the Afro-Arabian plate [e.g., Allen and Talebian, 2011], (2) the Upper Precambrian to Upper Devonian which is specified by the onset of subduction of the Palaeo-Tethys under the adjacent Gondwana margin [e.g., Orang *et al.*, 2018], (3) the Upper Devonian to Middle Permian event which is characterized by the continental rifting (Figure 1) and the opening of the Neo-Tethys Ocean (a new passive margin along the NE-Arabian plate margin) [e.g., Sharland *et al.*, 2004], (4) the Lower to Upper Cretaceous which is specified by the subduction of

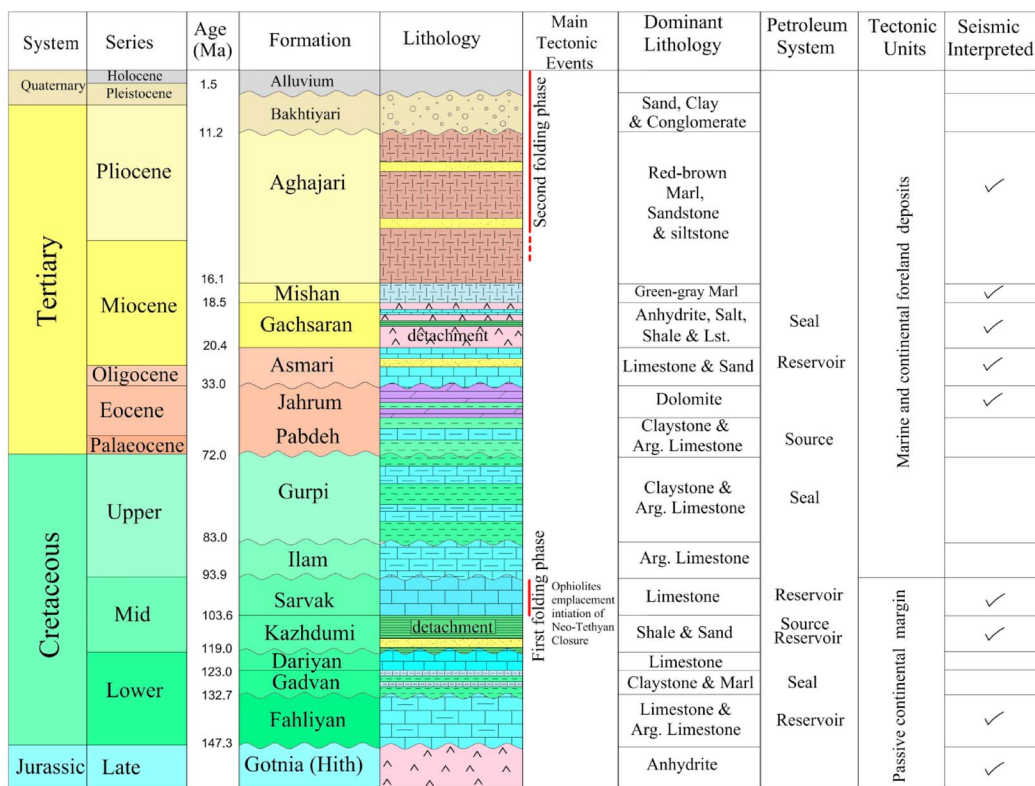


Figure 2. Stratigraphic column of the Upper Jurassic to Quaternary rock series in the Bahregansar anticline based on outcrop sections in the ZFTB and exploration wells showing key seismic horizons, major tectonic events, main lithologies, and petroleum systems [modified after Al-Husseini, 2008, Motiei, 1993].

the Neo-Tethys beneath the southern margin of the Eurasian plate [e.g., Agard et al., 2011, Mouthereau et al., 2012], and (5) the Miocene time which is specified by the continent–continent collision between the Eurasian and Afro-Arabian plates [McQuarrie, 2004]. At present, the convergence between these plates is still ongoing approximately in north–south directions [Lacombe et al., 2006, Agard et al., 2011, Mouthereau et al., 2006, 2012, Cai et al., 2021].

The present-day geometry of the Bahregansar anticline varies with depth. At deep levels (e.g., Upper Jurassic horizons of the Gotnia Formation), it is a large, elongated and NNE–SSW-trending anticlinal structure that has been affected and displaced by the HBNZ and also truncated by the Turonian angular unconformity (Figure 4). At shallower levels (e.g., Pliocene horizons of the Aghajari Formation), by contrast, it is a large, gentle, elongated and NW–SE-trending anticline (Figure 4). In the NE–SW-

trending depth section, the Pliocene strata dip 9° to the SW in the SW limb and 4° to the NE in the NE limb. Dip is approximately constant down section due to the effect of the HBNZ, so that the Lower Cretaceous formations have dip of 8° to the SE and 3° to the NW in the SE and NW limbs, respectively (Figures 4 and 5). In general, the Bahregansar anticline is interpreted as a gentle and elongated structure located in the NW Persian Gulf, which is also considered as an important reservoir.

The regional-scale simplified stratigraphic column of the Bahregansar anticline including formations, the dominant lithology, main tectonic events, source rocks, reservoirs cap rocks, tectonic units and interpreted seismic horizons are shown in the Figure 2. The stratigraphic column is based on outcrop sections in the ZFTB and exploration wells. Overall, the well-known rock intervals in the studied anticlinal structure range in age from the Up-

per Jurassic to the Quaternary. The Mesozoic sedimentary series consist of the Upper Jurassic Gotina Formation (mainly composed of anhydrite with some shale intervals), the Lower Cretaceous Garau and Fahliyan formations, the Albian Dariyan, the Upper Albian–Middle Turonian Sarvak, and the Santonian–Maastrichtian Ilam–Gurpi formations (argillaceous limestone, marl and limestone) and the Kazhdumi Formation (composed of shale, marl and sand) (Figure 2) [e.g., Motiei, 1993, Ghazban, 2007, Al-Husseini, 2008, Bahrehvar *et al.*, 2020]. Moreover, the Cenozoic sedimentary series include the Paleocene–Eocene Pabdeh Formation (composed of argillaceous limestone and marl), the Upper Eocene Jahrum Formation (composed of dolomitic limestone and dolomite), the Oligocene–Lower Miocene Asmari Formation (composed of limestone and sand), the Lower–Middle Miocene Gachsaran Formation (composed of anhydrite, salt, shale and limestone), the Lower–Middle Miocene Mishan Formation (composed of green/grey marl), the Upper Miocene–Pliocene Aghajari Formation (composed of red-brown marls and sand) and the Pliocene–Pleistocene Bakhtiyari Formation (composed of sand, clay and conglomerate) (Figure 2) [e.g., Motiei, 1993, Ghazban, 2007, Mouthereau *et al.*, 2007, Al-Husseini, 2008, Khadivi *et al.*, 2010, Bahrehvar *et al.*, 2020].

3. Materials and methods

In this study, the structural and stratigraphic analysis used an integrated dataset comprising high-quality 2D and 3D seismic data, well data and depth maps to consider and reconstruct the effects of the wrench-dominated basement-involved HBNF on folding of the overlying sedimentary sequences and the structural evolution in the Bahregansar anticline (Figure 3). High-quality 3D seismic cube together with several 2D seismic sections from the Bahregansar field are provided by an approximately 380 km² dual sensor Ocean Bottom Cable (OBC) survey recorded during 2006 to 2008 and reprocessed in Iranian Offshore Oil Company in 2012. Furthermore, the interpretation of the formation tops and faults were done in the depth domain.

Seismic interpretation was undertaken using Schlumberger's Petrel 2018 software. Prominent reflections were mapped across the studied structure

with a focus on the top of formations. To do so, the relationship between time and depth was obtained from exploration wells using synthetic seismograms to associate the relevant seismic reflectors with their depth and corresponding stratigraphy. The 2D sequential restoration was performed using 2D Midland Valley Move 2018 software on top of 10 formations and 4 faults, respectively, by flexural slip and fault parallel flow algorithms [e.g., Griffiths *et al.*, 2002] in order to reconstruct the structural evolution of the Bahregansar anticline. The selected cross section for restoration is perpendicular to the axial plane of the Bahregansar anticline and parallel to the shortening direction applied to the wrench-dominated basement-involved fault. At each stage of reconstruction, the youngest sedimentary Formation was unfaulted and the unfolded. The assumptions for the sequential restoration are: (1) the layers were horizontally deposited, hence the effect of palaeo-high slopes were not considered; (2) decompaction was not done in the study area due to the carbonate and argillaceous limestone lithologies with low compaction; (3) the amount of removed sediments were not considered due to the unavailability of the erosion rate of the main unconformities occurred in the area; (4) the Bahregansar anticline is developed by horizontal shortening during the folding phase.

4. Results

4.1. Structural maps and seismic reflection interpretation

Seven representative depth maps for the tops of the Upper Jurassic to Pliocene formations (Figures 4a–g) show the present-day geometry of the Bahregansar anticline varies with depth. For a better comparison, the scale ranges of all the structural maps are the same. Regarding the structural maps of Asmari to the Gotina Formation and occurrence of a pull-apart basin at the tops of the Asmari and Jahrum formations (Figures 4c,d and 5), the offsets of the contours display the trace of the HBNF and the red line with arrows illustrates the last strike-slip displacement of this fault. The trend of the Bahregansar anticline in the younger sediments (i.e., from the Aghajari Formation to the Sarvak Formation) is NW–SE (Zagros trend), however, its trend changed to N–S in the older deposits (i.e., from the Kazhdumi Formation to

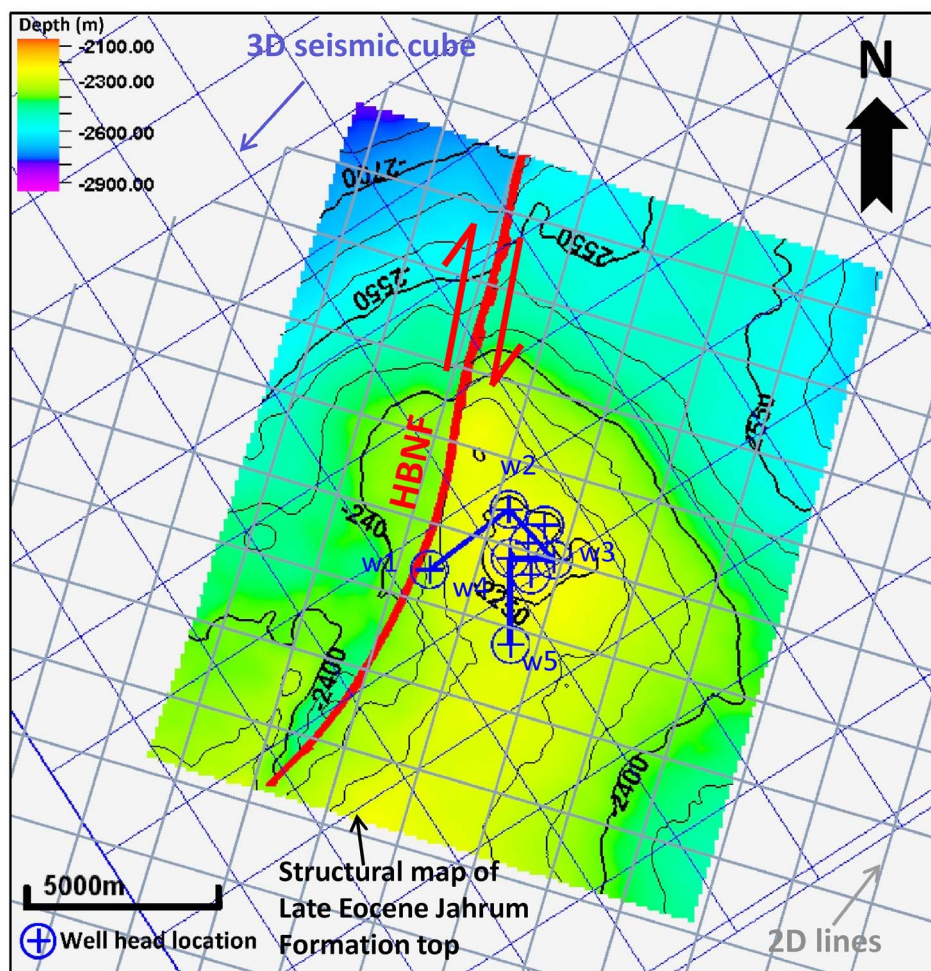


Figure 3. The surface pattern of the 2D seismic profile and the 3D seismic cube used in the Bahregansar anticline. The structural map (the top of the Upper Eocene Jahrum Formation) shows the location of exploration wells in the study area.

the Gotnia Formation) (Arabian trend) and parallel to the HBNF (Figure 4). Furthermore, two pull-apart structures can be recognized in the southwest of the Bahregansar anticline and adjacent to the HBNF on the structural maps of the Asmari and Jahrum formation tops (Figures 4c,d and 5). These pull-aparts are structural depressions where two interacting strike-slip fault segments of the HBNF zone create an extensional overlap (Figure 5). According to previous studies [e.g., Berberian, 1995, Bahroudi and Talbot, 2003, Mohammadrezaei *et al.*, 2020] the last kinematics of the HBNF is considered to be a dextral movement.

Six main seismic reflectors trace also across large portions of the Bahregansar anticline (Figure 4h).

Seismic interpretation helped to constrain the different structural geometries with the studied anticline and the effect of the basement structure on overlying sedimentary strata. Integrating the seismic reflection data with structural depth maps and well data increased confidence in the interpretation and gave insights on the structural evolution of the structure at different scale of observation. In the interpreted serial seismic cross sections, the key formation tops, growth strata, angular unconformity, detachment units and the HBNF with minor faults are displayed (Figure 4). A series of seismic profiles along and across the Bahregansar anticline show the variation in the structural style from northeast to

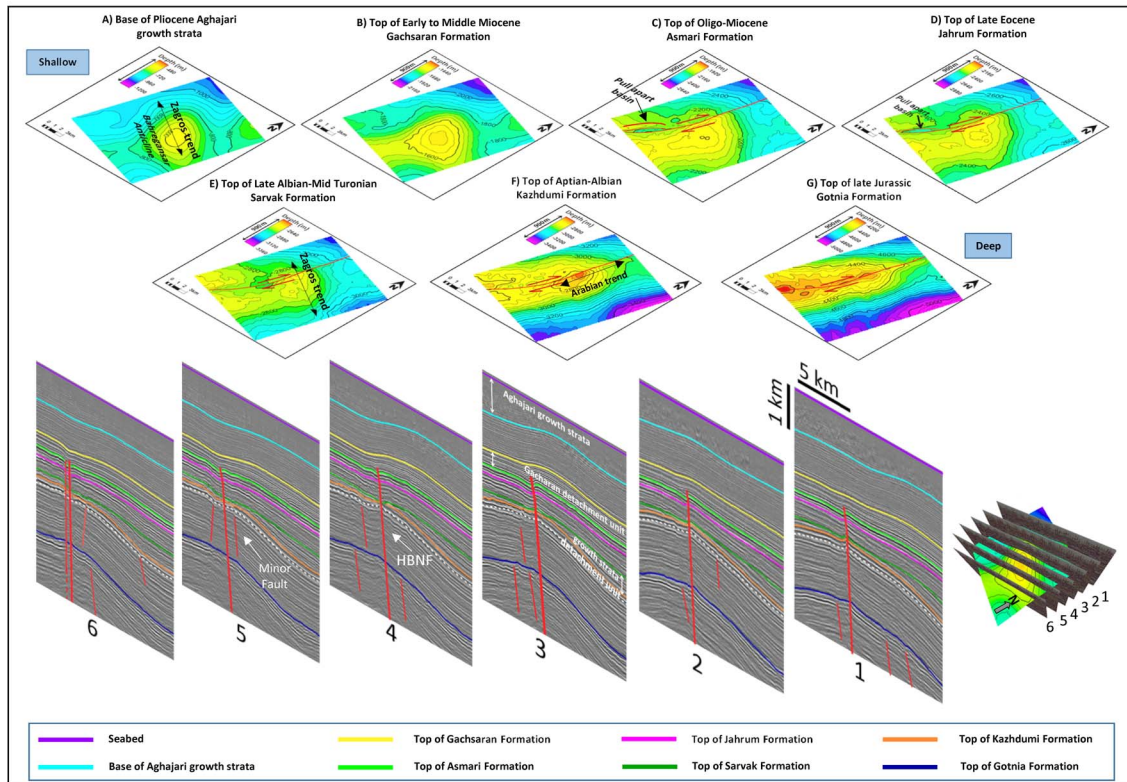


Figure 4. The structural maps (the top of the Upper Jurassic Gotnia Formation to the base of Pliocene Aghajari growth strata) in the Bahregansar anticline based on the interpretation of seismic profiles across the studied anticline. Pull-apart basins, as a key structural element, can be clearly seen on the structural maps of the Asmari and Jahrum formations tops, and illustrating the dextral sense of displacement along the HBNF. Furthermore, some key features such as formation tops, the HBNF, growth strata, and detachment levels can be clearly observed on the serial seismic sections. The vertical exaggeration of these sections is 5. The inset illustrates the seismic sections on the structural map of the Jahrum Formation. The seismic section 3 has been selected for sequential restoration.

southwest, with the wrench-dominated basement-involved fault rooted in the Upper Jurassic Gotnia Formation having significant effect on the folding of overlying sedimentary strata (Figure 4). The strike, dip angle and throw of fault segments along their trend and trace change between seismic lines so that the amount of deformation stage and strain vary between layers. Overall, the older and younger sets of the minor faults are mostly restricted to the Gotnia Formation and the Kazhdumi detachment levels, respectively. The variability of fault geometry and fold style indicates that the central portion of the basement fault are affect by several fault segments. The minor faults have various dips from 70° to 85° (Figure 4).

4.2. Analysis of vertical thickness maps and sequential restored sections

Figure 6 demonstrates the vertical thickness maps (from the Pliocene to the Lower Cretaceous) and the sequential restoration section of formation tops and the HBNF across the Bahregansar anticline. According to the vertical thickness maps, the Sarvak and Aghajari growth strata can be clearly recognized by the decreasing the sedimentary thickness towards the flanks of the Bahregansar anticline (Figure 6). Moreover, it should be noted that the Aghajari growth strata displays the Zagros trend (i.e., NNW–SSE), whereas the Sarvak growth strata obviously shows the Arabian trend and parallel to the HBNF

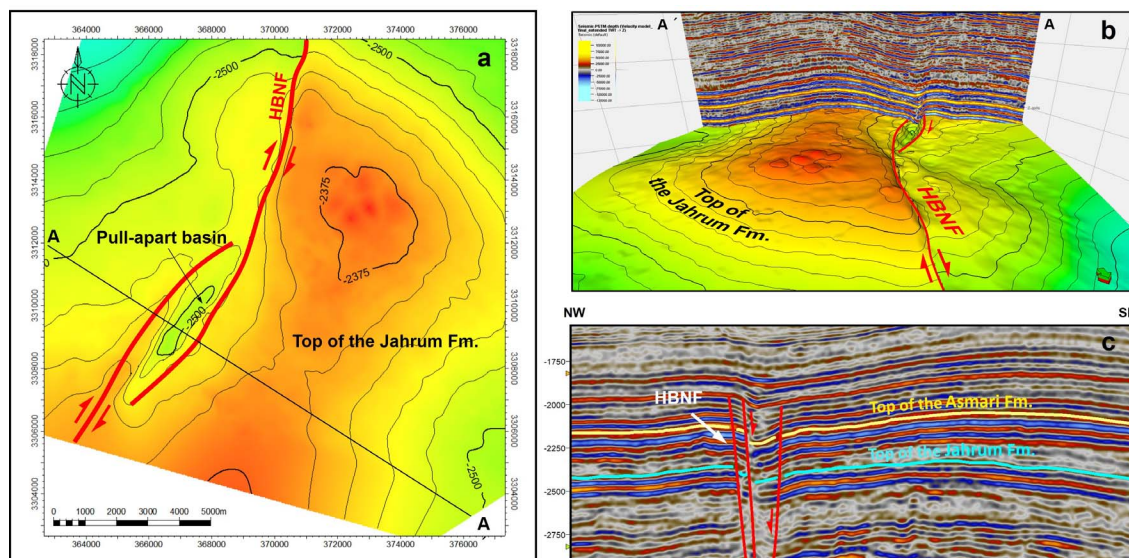


Figure 5. (a) The structural map derived from the top of the Upper Eocene Jahrum Formation along the Bahregansar anticline shows that the pull-apart basin resulted from two right-stepping, interacting, overlapping dextral fault segments of the HBNF and the location of the seismic section AA' is presented in (b) and (c). (b) 3D view of the developed pull-part basin and associated depression, as a key structural feature, at the top of the Upper Eocene Jahrum Formation within two right-stepping, interacting, overlapping dextral fault segments of the HBNF, which they also interpreted in the seismic section AA'. (c) Fault interpretation of the seismic section AA' showing the depressed portions within the developed pull-apart basin in the Asmari and Jahrum formations.

(i.e., NNE–SSW) (Figures 4 and 6). The isochores of Aghajari and Mishan formations indicate a preferential Zagros trend. However, the isochores illustrate a predominant Arabian trend parallel to the HBNF from the Gachsaran Formation downward to the Fahliyan Formation (Figure 6). In the southwestern part of the vertical thickness map and the vicinity of the HBNF, the variations of the isochore values, as the key points, have been marked by a dotted elliptical shape (A) (Figure 6). These lower isochore values (i.e., dotted elliptical shape) suggest uplift or push-up blocks along the HBNF which were developed between overlapping fault segments and caused the localization of contraction and positive topography along the HBNF zone. It is interpreted that the basement-involved fault zone controlled the uplifted and subsided parts within the study area and thus the thickness and facies distribution of the sedimentary sequences mentioned in the Bahregansar anticline. Furthermore, such push-up blocks which correspond to the pull-apart basins (Figure 5), are marked by sinistral movement along the HBNF dur-

ing the Lower Cretaceous to the Upper Eocene. The comparison of the pull-apart basins and push-up blocks suggested that the kinematics of the HBNF in the Bahregansar anticline had switched from sinistral to dextral sense of displacement in response to the Zagros orogeny.

The sequential restoration of a section across the Bahregansar anticline is shown in the Figure 6. The HBNF was modelled to understand the control of basement-involved faults in the Bahregansar anticline on overlying sedimentary strata using the high-quality 3D seismic data across the structure. The geometry of the existing sedimentary basin with the last offsets of deposits (due to the last activities of the HBNF) has been shown in stage 1 (Figure 6). The most growth of the Bahregansar anticline has occurred during the sedimentation of the Pliocene Aghajari Formation. Stages 2 and 3 illustrate the restorations to the tops of Mishan and Gachsaran formations, respectively. Stage 4 indicates the restoration to the top of the Asmari Formation that includes removing 30 m reverse displacement on the HBNF.

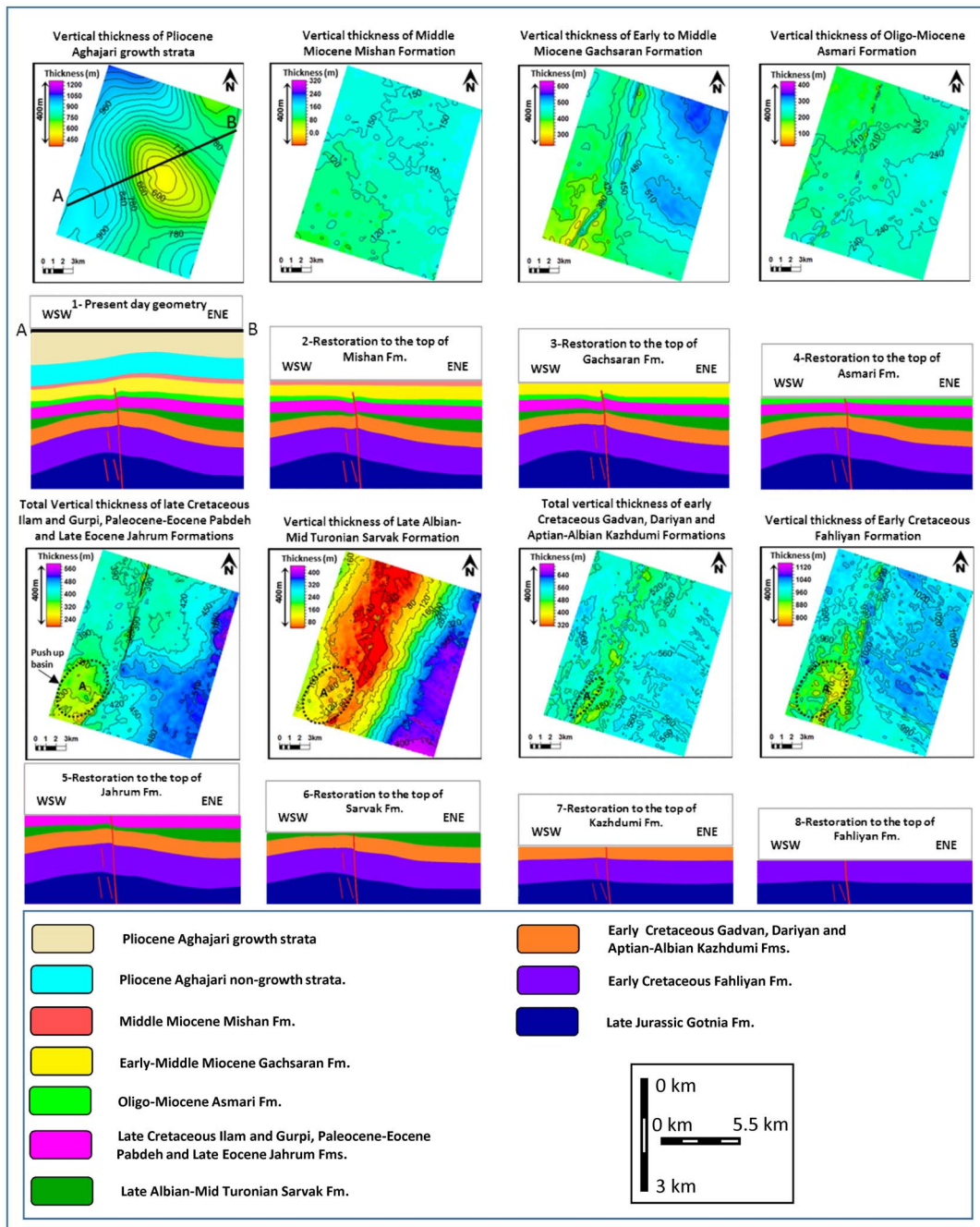


Figure 6. Eight representative thickness maps (isochores) of the Pliocene to Lower Cretaceous sedimentary strata in the Bahregansar anticline. Sequential restoration of a NE–SW-trending depth at a perpendicular across the Bahregansar anticline based on the seismic line 3. Push-up structures (marked by a dashed oval marked by A) have been identified on several vertical thickness maps so that such structural features illustrate the sinistral sense of displacement along the HBNE, which cross-cuts the Lower Cretaceous to Upper Eocene strata. According to sequential restoration, two folding phases and two different dip-slip components (normal and reverse slip) are also identified in the Bahregansar anticline.

Stage 5 shows restoration to the top of the Jahrum Formation. Stage 6 illustrates the restoration to the top of the Sarvak Formation that involves removing 23 m reverse movement on the fault. This stage represents the growth strata of the Sarvak Formation. Stage 7 shows the restoration to the top of the Kazhdumi Formation that involves removing 10 m normal movement on the fault. Stage 8 illustrates the restorations to the tops of the Fahliyan Formation that include removing 22 m normal movements on the HBNF (Figure 6). Axial surface of the fold structure is initially upright, then tends to become progressively inclined with an external vergence, forming an asymmetric deformation zone localized on the wrench-dominated basement-involved HBNF. The detachment level of the Gachsaran Formation caused the propagating tip and associated fault throw of the HBNF to die out within it, and hence, the fault no longer appears within the upper strata, but is guided by the trend of the underlying fault in the form of buckle fold development.

5. Discussion

Definition of the structural style of the tectonic setting and understanding the controlling factors are necessary steps toward prediction of their geometry, kinematics and dynamics and to assess their potential in terms of hydrocarbon exploration. The structural evolution and style of a faulted strata are determined by its geometric, kinematic, and rheological characteristics. However, fault kinematics obviously reflect the local and regional stress field and also tectonic setting. Development of basement-involved faulting requires repeated throughgoing failure of the basement to initiate new structures or to reactivate pre-existing structures. Reactivation of high-angle structures at depth in an obliquely converging setting can cause deformation to propagate upward as a partitioned system of oblique-slip faults and associated folding, potentially representing a lower stress distribution and strain localization conditions [e.g., Nabavi *et al.*, 2018, 2020]. Seismic data confirm that the major fault system of the HBNF affecting the Bahregansar anticline is the wrench-dominated basement-involved fault system with a dextral transpressive deformation, which is oriented with NE–SE strike. The major fault was interpreted as a continuous and high-angle fault plane with some

discontinuous and segmented minor fault planes due to their variable geometries along and across the trend of the structure. The integration of seismic reflection and well data as well as thickness maps suggests that the geometric and kinematic variability of the wrench-dominated basement-involved HBNF had a significant control over the depositional evolution, stratigraphic continuity, facies distribution, and subsequent structural evolution and folding deformation of the overlying sedimentary sequences. However, some faults did not propagate upwards, or were slightly reactivated, and therefore had little influence on the sedimentary succession in the study area and the evolution of the anticline.

Two active detachment levels including the Albian Kazhdumi shale Formation and the Miocene Gachsaran evaporites Formation extended in to the Bahregansar anticline. On the NW–SE-trending interpreted seismic lines and according to the present geometry of the Bahregansar anticline (Figure 7), the attitude and geometry of the Aghajari growth strata (Pliocene) are in accordance with a regional shortening direction of NE–SW, whereas the geometry of the Sarvak Formation is consistent with the applied shortening direction of E–W. This change in the structural trend of the Bahregansar anticline has been suggested to be due to the Kazhdumi shale Formation, which is an important detachment level in the area, that led to the decoupling of deformation in the overlying sedimentary strata and underlying ones (Figure 4). Strike-slip fault systems can be divided into four groups, depending on whether the master fault dies out within the basement (thick-skinned) or within the salt or incompetent layer (thin-skinned) and whether a precursor diapir is present before strike-slip begins [Jackson and Hudec, 2017]. In this regard, structure maps and seismic reflection sections (Figure 4) imply that the propagating tip and associated fault throw of the HBNF died out within the Gachsaran evaporites Formation. This characteristic indicates that the evaporitic Gachsaran Formation has acted as an active detachment level that led to the decoupling of deformation in the overlying sedimentary strata, which are geometrically unaffected by the HBNF, and underlying ones such as Hith/Gotnia Formation to the Ghachsaran Formation, which are geometrically affected and displaced by the HBNF movements. The effects of detachment levels mentioned above on folding, faulting, and the

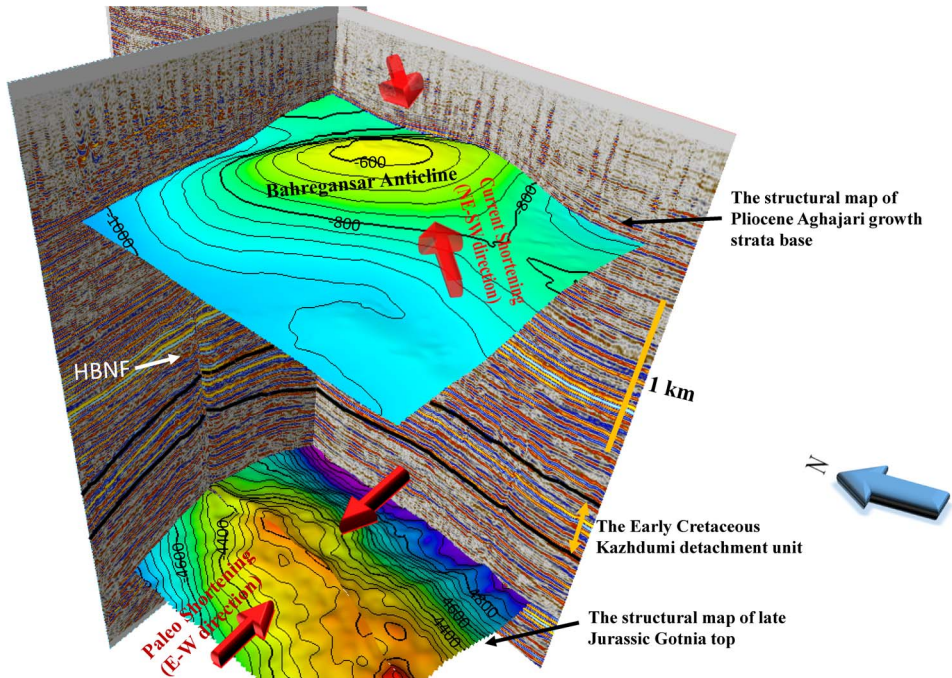


Figure 7. 3D view of the HBNF and Bahregansar anticline shows two different trends of fold axes such as the Arabian- and Zagros-trends in the study area. The shortening directions are shown in red arrows.

structural style of the area are also reported in the Persian Gulf and the ZFTB onshore area [e.g., Mohammadrezaei *et al.*, 2020, Karimnejad Lalami *et al.*, 2020, Ghanadian *et al.*, 2017b,c, Soleimany and Sàbat, 2010].

Restoration results and seismic interpretations indicate a kind of basement-involved high-angle fault reactivation in the Bahregansar anticline, where the sinistral-normal HBNF fault developed up to the Middle Cretaceous. In the Upper Cretaceous, the HBNF propagated upward through the overlying sedimentary sequences when the inherited normal fault contractionally reactivated in sinistral-reverse sense, as the transpression zone [e.g., Viola *et al.*, 2004], in response to the Neo-Tethys oceanic plate subduction under the Eurasian plate. In this regard, the NNE–SSW-trending Bahregansar anticline (i.e., Arabian trend) formed as a forced fold. This result is also supported by several studies in the Persian Gulf and the ZFTB onshore area [e.g., Shi-roodi *et al.*, 2015, Mohammadrezaei *et al.*, 2020, Sattarzadeh *et al.*, 1999]. Continuing oblique convergence and associated deformation was accommodated by a change in the HBNF displacement sense

from sinistral to dextral movement and buckling of the Bahregansar anticline as a result of the Pliocene Zagros orogeny in accordance with previous studies in the ZFTB area [e.g., Mohammadrezaei *et al.*, 2020, Soleimany and Sàbat, 2010]. Overall, oblique slip along the basement-involved fault is usually accommodated in the cover by a triangular, widening-upward deformation zone on the forelimb with the nature of deformation controlled by the mechanical stratigraphy. These resulted in low amplitude monoclinical geometry of the Bahregansar anticline with low magnitude thinning of hanging wall and thickening of footwall blocks. In this regard, we found that deformation along the basement fault is propagated up the cover over three structural domains: (1) basal wrench-dominated faulted block, (2) middle faulted monoclinical forced fold that transitions into (3) monoclinical buckle fold of the overlying sedimentary strata. Overall, three processes and factors were involved in the nucleation, development and evolution of the Bahregansar anticline including the activation and reactivation of the HBNF in different stages, and the effect of detachment levels (Figure 6). Moreover, it seems likely that the interaction between

processes mentioned above controlled the thickness of sedimentary strata in the Bahregansar structure (Figure 6).

6. Conclusions

Interpretation of seismic reflection profiles, well data as well as thickness and deep maps reveal a clear wrench-dominated basement-involved structural framework (i.e., the HBNF) rooted in the NW Persian Gulf that affected the folding of overlying sedimentary strata (i.e., the Bahregansar anticline) in both the geometry and kinematics of the structure as well as in the thickness and facies variations. The results show that the major basement-involved fault of the HBNF extends along the NE–SW-trending orientation and consists of several key anticlines.

The structural evolution of the Bahregansar anticline has been deeply affected by the Turonian folding phase and Pliocene Zagros orogeny associated with the HBNF. In the Upper Cretaceous, the HBNF propagated upward through the overlying sedimentary sequences when the inherited normal fault contractionally reactivated, as the transpression zone, in sinistral-reverse sense in response to the Neo-Tethyan oceanic plate subduction under the Eurasian plate. In this regard, the NNE–SSW-trending Bahregansar anticline (i.e., Arabian trend) formed as a forced fold. Continuing oblique convergence and associated deformation was accommodated by a change in the HBNF displacement sense from sinistral to dextral and by buckling of the Bahregansar anticline as a result of the Pliocene Zagros orogeny.

Overall, we found that deformation along the basement fault is propagated up the cover over three structural domains: (1) basal wrench-dominated faulted block, (2) middle faulted monoclinical forced fold that transitions into (3) monoclinical buckle fold of the overlying sedimentary strata. An understanding of the geometry and kinematics of basement faults within hydrocarbon provinces is therefore a valuable predictive tool in exploration. Furthermore, we demonstrated that the basement-involved fault propagation has greater efficiency of propagating the fault-related deformation to shallower depths compared to the intrasedimentary-driven nucleation and propagation.

Conflicts of interest

Authors have no conflict of interest to declare.

Acknowledgements

The authors thank the Faculty of Earth Sciences at Shahid Beheshti University for its support of the present work. Our thanks are also extended to the Iranian Offshore Oil Company (IOOC) for providing the subsurface data, facilities, and permission to publish some well data and the interpretation of some seismic data. We are also grateful to Professor Nestor Cardozo and Dr Seyed Tohid Nabavi for their constructive reviews, suggestions and comments in improving this manuscript. We thank reviewer Professor Frederick Mouthereau for constructive review, comments and helpful suggestions which allowed us to improve the original manuscript. Editorial and handling efforts by François Chabaux are also gratefully acknowledged.

References

- Agard, P., Omrani, J., Jolivet, L., Whitechurch, H., Vrielynck, B., Spakman, W., Monié, P., Meyer, B., and Wortel, R. (2011). Zagros orogeny: a subduction-dominated process. *Geol. Mag.*, 148, 692–725.
- Al-Husseini, M. (2008). Middle east geological time scale 2008: cenozoic Era, cretaceous and jurassic periods of mesozoic Era. *GeoArabia*, 13, 185–188.
- Allen, M. B. and Talebian, M. (2011). Structural variation along the Zagros and the nature of the Dezful Embayment. *Geol. Mag.*, 148, 911–924.
- Bahrehvar, M., Mehrabi, H., and Rahimpour-Bonab, H. (2020). Coated grain petrography and geochemistry as palaeoenvironmental proxies for the Aptian strata of the southern Neo-Tethys Ocean, Persian Gulf, Iran. *Facies*, 66, article no. 3.
- Bahroudi, A. and Talbot, C. J. (2003). The configuration of the basement beneath the Zagros Basin. *J. Petrol. Geol.*, 26, 257–282.
- Berberian, M. (1995). Master “blind” thrust faults hidden under the Zagros folds: active basement tectonics and surface morphotectonics. *Tectonophysics*, 241(3-4), 193–224.
- Cai, F., Ding, L., Wang, H., Laskowski, A. K., Zhang, L., Zhang, B., Mohammadi, A., Li, J., Song, P., Li, Z.,

- and Zhang, Q. (2021). Configuration and timing of collision between Arabia and Eurasia in the Zagros collision zone, Fars, southern Iran. *Tectonics*, 40(8), article no. 2021TC006762.
- Cooper, S. P., Goodwin, L. B., and Lorenz, J. C. (2006). Fracture and fault patterns associated with basement-cored anticlines: the example of Teapot Dome, Wyoming. *AAPG Bull.*, 90, 1903–1920.
- Edgell, H. S. (1996). Salt tectonism in the Persian Gulf basin. *Geol. Soc. Lond. Spec. Publ.*, 100, 129–151.
- Ghanadian, M., Faghih, A., Fard, I. A., Grasemann, B., Soleimany, B., and Maleki, M. (2017a). Tectonic constraints for hydrocarbon targets in the Dezful embayment, Zagros Fold and Thrust Belt, SW Iran. *J. Petrol. Sci. Eng.*, 157, 1220–1228.
- Ghanadian, M., Faghih, A., Fard, I. A., Kusky, T., and Maleki, M. (2017c). On the role of incompetent strata in the structural evolution of the Zagros Fold-Thrust Belt, Dezful Embayment, Iran. *Mar. Pet. Geol.*, 81, 320–333.
- Ghanadian, M., Faghih, A., Grasemann, B., Fard, I. A., and Maleki, M. (2017b). Analogue modeling of the role of multi-level decollement layers on the geometry of orogenic wedge: an application to the Zagros Fold–Thrust Belt, SW Iran. *Int. J. Earth Sci.*, 106, 2837–2853.
- Ghazban, F. (2007). *Petroleum Geology of the Persian Gulf*. Tehran University Press and National Iranian Oil Company, Tehran, Iran.
- Granado, P., Thöny, W., Carrera, N., Gratzner, O., Strauss, P., and Muñoz, J. A. (2016). Basement-involved reactivation in foreland fold-and-thrust belts: the Alpine-Carpathian Junction (Austria). *Geol. Mag.*, 153, 1110–1135.
- Griffiths, P., Jones, S., Salter, N., Schaefer, F., Osfield, R., and Reiser, H. (2002). A new technique for 3-D flexural-slip restoration. *J. Struct. Geol.*, 24, 773–782.
- Jackson, M. P. and Hudec, M. R. (2017). *Salt Tectonics: Principles and Practice*. Cambridge University Press, Cambridge, UK.
- Karimnejad Lalami, H. R., Hajjalibeigi, H., Sherkati, S., and Adabi, M. H. (2020). Tectonic evolution of the Zagros foreland basin since Early Cretaceous, SW Iran: regional tectonic implications from subsidence analysis. *J. Asian Earth Sci.*, 204, article no. 104550.
- Khadivi, S., Mouthereau, F., Larrasoana, J.-C., Vergés, J., Lacombe, O., Khademi, E., Beamud, E., Melinte-Dobrinescu, M., and Suc, K.-P. (2010). Magnetostratigraphy of synorogenic Miocene foreland sediments in the Fars arc of the Zagros Folded Belt (SW Iran). *Basin Res.*, 22, 918–932.
- Konyuhov, A. I. and Maleki, B. (2006). The Persian Gulf Basin: geological history, sedimentary formations, and petroleum potential. *Lithol. Miner. Resour.*, 41, 344–361.
- Koyi, H. A., Ghasemi, A., Hessami, K., and Dietl, C. (2008). The mechanical relationship between strike-slip faults and salt diapirs in the Zagros fold-thrust belt. *J. Geol. Soc.*, 165, 1031–1044.
- Lacombe, O. and Bellahsen, N. (2016). Thick-skinned tectonics and basement-involved fold-thrust belts: insights from selected Cenozoic orogens. *Geol. Mag.*, 153, 763–810.
- Lacombe, O., Mouthereau, F., Kargar, S., and Meyer, B. (2006). Late Cenozoic and modern stress fields in the western Fars (Iran): implications for the tectonic and kinematic evolution of central Zagros. *Tectonics*, 25, 1–27.
- McClay, K. R. (2011). Introduction to thrust fault-related folding. In McClay, K. R., Shaw, J., and Suppe, J., editors, *Thrust Fault-Related Folding*, volume 94 of *AAPG Memoir*, pages 1–19. American Association of Petroleum Geologists, USA.
- McClay, K. R. and Ellis, P. G. (1987). Geometries of extensional fault systems developed in model experiments. *Geology*, 15, 341–344.
- McQuarrie, N. (2004). Crustal scale geometry of the Zagros fold-thrust belt, Iran. *J. Struct. Geol.*, 26, 519–535.
- Mitra, S. and Mount, V. S. (1998). Foreland basement-involved structures. *AAPG Bull.*, 82, 70–109.
- Mohammadrezaei, H., Alavi, S. A., Cardozo, N., and Ghassemi, M. R. (2020). Deciphering the relationship between basement faulting and two-phase folding in the Hendijan anticline, northwest Persian Gulf, Iran. *Mar. Pet. Geol.*, 122, article no. 104626.
- Molinario, M., Guezou, J. C., Leturmy, P., Eshraghi, S. A., and de Lamotte, D. F. (2004). The origin of changes in structural style across the Bandar Abbas syntaxis, SE Zagros (Iran). *Mar. Pet. Geol.*, 21, 735–752.
- Motiei, H. (1993). *Stratigraphy of Zagros, Treatise on the geology of Iran*. Geological Survey of Iran 160, Tehran, Iran. (in Persian).
- Mouthereau, F., Lacombe, O., and Meyer, B. (2006).

- The Zagros folded belt (Fars, Iran): constraints from topography and critical wedge modelling. *Geophys. J. Int.*, 165, 336–356.
- Mouthereau, F., Lacombe, O., and Vergés, J. (2012). Building the Zagros collisional orogen: timing, strain distribution and the dynamics of Arabia/Eurasia plate convergence. *Tectonophysics*, 532, 27–60.
- Mouthereau, F., Tensi, J., Bellahsen, N., Lacombe, O., De Boisgrollier, T., and Kargar, S. (2007). Tertiary sequence of deformation in a thin-skinned/thick-skinned collision belt: the Zagros folded Belt (Fars, Iran). *Tectonics*, 26, 1–28.
- Nabavi, S. T., Alavi, S. A., Díaz-Azpiroz, M., Mohammadi, S., Ghassemi, M. R., Fernández, C., Barcos, L., and Frehner, M. (2020). Deformation mechanics in inclined, brittle-ductile transpression zones: insights from 3D finite element modelling. *J. Struct. Geol.*, 137, article no. 104082.
- Nabavi, S. T., Alavi, S. A., Mohammadi, S., and Ghassemi, M. R. (2018). Mechanical evolution of transpression zones affected by fault interactions: insights from 3D elasto-plastic finite element models. *J. Struct. Geol.*, 106, 19–40.
- Neng, Y., Xie, H., Yin, H., Li, Y., and Wang, W. (2018). Effect of basement structure and salt tectonics on deformation styles along strike: an example from the Kuqa fold–thrust belt, West China. *Tectonophysics*, 730, 114–131.
- Orang, K., Motamedi, H., Azadikhah, A., and Royatvand, M. (2018). Structural framework and tectono-stratigraphic evolution of the eastern Persian Gulf, offshore Iran. *Mar. Pet. Geol.*, 91, 89–107.
- Pirouz, M., Simpson, G., Bahroudi, A., and Azhdari, A. (2011). Neogene sediments and modern depositional environments of the Zagros foreland basin system. *Geol. Mag.*, 148, 838–853.
- Sarkarinejad, K. and Goftari, F. (2019). Thick-skinned and thin-skinned tectonics of the Zagros orogen, Iran: constraints from structural, microstructural and kinematics analyses. *J. Asian Earth Sci.*, 170, 249–273.
- Sattarzadeh, Y., Cosgrove, J. W., and Vita-Finzi, C. (1999). The interplay of faulting and folding during the evolution of the Zagros deformation belt. *Geol. Soc. Lond. Spec. Publ.*, 169, 187–196.
- Sepehr, M. and Cosgrove, J. W. (2007). The role of major fault zones in controlling the geometry and spatial organization of structures in the Zagros fold–thrust belt. *Geol. Soc. Lond. Spec. Publ.*, 272, 419–436.
- Sharland, P. R., Casey, D. M., Davies, R. B., Simmons, M. D., and Sutcliffe, O. E. (2004). Arabian plate sequence stratigraphy—revisions to SP2. *GeoArabia*, 9, 199–214.
- Shiroodi, S. K., Ghafoori, M., Faghieh, A., Ghana-dian, M., Lashkaripour, G., and Moghadas, N. H. (2015). Multi-phase inversion tectonics related to the Hendijan–Nowrooz–Khafji Fault activity, Zagros Mountains, SW Iran. *J. Afr. Earth Sci.*, 111, 399–408.
- Soleimany, B. and Sàbat, F. (2010). Style and age of deformation in the NW Persian Gulf. *Petrol. Geosci.*, 16, 31–39.
- Viola, G., Odonne, F., and Mancktelow, N. S. (2004). Analogue modelling of reverse fault reactivation in strike–slip and transpressive regimes: application to the Giudicarie fault system, Italian Eastern Alps. *J. Struct. Geol.*, 26, 401–418.
- Wang, C., Cheng, X., Chen, H., Ding, W., Lin, X., Wu, L., Li, K., Shi, J., and Li, Y. (2016). The effect of foreland palaeo-uplift on deformation mechanism in the Wupoer fold-and-thrust belt, NE Pamir: constraints from analogue modelling. *J. Geodynam.*, 100, 115–129.